

# Using current surface probe to measure the current of the fast power semiconductors

**Li, K., Videt, A. & Idir, N.**

Author post-print (accepted) deposited by Coventry University's Repository

**Original citation & hyperlink:**

Li, K, Videt, A & Idir, N 2015, 'Using current surface probe to measure the current of the fast power semiconductors' IEEE Transactions on Power Electronics, vol. 30, no. 6, 6965614, pp. 2911-2917.

<https://dx.doi.org/10.1109/TPEL.2014.2373400>

DOI 10.1109/TPEL.2014.2373400

ISSN 0885-8993

ESSN 1941-0107

Publisher: IEEE

**© 2015 IEEE. Personal use of this material is permitted. Permission from IEEE must be obtained for all other uses, in any current or future media, including reprinting/republishing this material for advertising or promotional purposes, creating new collective works, for resale or redistribution to servers or lists, or reuse of any copyrighted component of this work in other works.**

**Copyright © and Moral Rights are retained by the author(s) and/ or other copyright owners. A copy can be downloaded for personal non-commercial research or study, without prior permission or charge. This item cannot be reproduced or quoted extensively from without first obtaining permission in writing from the copyright holder(s). The content must not be changed in any way or sold commercially in any format or medium without the formal permission of the copyright holders.**

**This document is the author's post-print version, incorporating any revisions agreed during the peer-review process. Some differences between the published version and this version may remain and you are advised to consult the published version if you wish to cite from it.**

# Using Current Surface Probe to Measure the Current of the Fast Power Semiconductors

Ke LI, *IEEE Member*, Arnaud VIDET, *IEEE Member*, Nadir IDIR, *IEEE Member*  
(ke1.li@ed.univ-lille1.fr; arnaud.videt@univ-lille1.fr; nadir.idir@univ-lille1.fr)

**Abstract**—With the advantage of high bandwidth and small insertion impedance, a current surface probe (CSP) used to measure switching current waveforms is presented in this letter. Its transfer impedance is characterized and validated by measuring an IGBT switching current that is compared with those obtained with a current probe (CP) and a Hall effect current probe (HECP). Furthermore, by comparing with a current shunt (CS) to measure a GaN-HEMT switching current, it is shown that CSP is able to measure a switching current of a few nanoseconds, while it brings no influence on transistor voltage waveform measurement. The obtained results show that, the use of CSP brings little parasitic inductances in the measurement circuit and it does not bring the connection of the ground to the power converter.

**Index Terms**—Gallium Nitride (GaN), Fast switching current, Current measurement, Current surface probe, Probe transfer impedance, Current Shunt.

## I. INTRODUCTION

WIDE bandgap power devices are gradually used in power electronic systems to achieve high power efficiency [1]–[4], high frequency [5], [6] and high operating temperature [7]. In a traditional power converter with silicon (Si) transistor, current switches during several tens to hundreds of nanoseconds [8], while with GaN transistors, the current transitions may be shortened to a few nanoseconds [9], [10]. This evolution requires that the current measurement probes are with high bandwidth and with small insertion impedances. It is well known that the current probes insertion impedance in the measurement circuit may modify the current switching waveforms [11]. Among the current measurement techniques presented by authors in [12], [13], at present, there are Hall Effect Current Probe (HECP), Rogowski Coil (RC) and Current Shunt (CS) that are mainly used to measure power devices switching current of power converters. The advantages and drawbacks of those current measurement equipments are summarized in the following paragraph.

- Hall Effect Current Probe (HECP): it is an active current probe with the advantage that it is able to measure DC current. The maximum bandwidth of a commercial HECP nowadays can reach up to 120MHz, with a maximum measurement DC current up to 30A. However, this probe brings an insertion impedance in the measurement power circuit, which may have influence on both switching current and switching voltage waveforms. Otherwise, the HECP maximum measurement current decreases with the frequency increase [14]. According to their technical datasheets, the maximum value generally decreases to

a factor of 6 above 10MHz. Thus, it is difficult to use a HECP to measure GaN-HEMT switching current waveform during a few nanoseconds.

- Rogowski Coil (RC): the main advantage of this probe is that there is no saturation phenomenon because it does not use magnetic materials [15]. Another advantage of the RC is that its volume is small, so it brings almost no insertion impedance on the measurement circuit. No special current measurement circuit is necessary, because it can be wound around one leg of the power device. Therefore, the commutation mesh of the power devices when using this probe is small. However, the main drawback is that the commercial RC is limited at a maximum frequency of 30MHz, which equals to the current switching time of 10ns.
- Current Shunt (CS): it is nowadays widely used for fast switching current measurement. Authors in [10], [16], [17] used the CS to measure SiC-JFET and GaN-HEMT switching current. The advantage of the CS is that it has a large bandwidth (above 1GHz), which makes it totally adapted for the fast switch power semiconductors. However, the CS links the ground of the oscilloscope to the measurement power circuit, in which special cautions must be taken when another ground connection equipment is used in the circuit (in case of simultaneous current measurement by CS). This drawback also introduces a hard-to-be-controlled common mode loop of the circuit (modification of the circuit potentials and the common mode current paths), which may influence the measurement results. It can be also noted that there is no isolation between the CS and the oscilloscope and its insertion impedance can vary from several to more than a dozen  $nH$  according to different models [16], [17]. Besides that, the heating can become also a problem of the CS [18].

Apart from the above current measurement equipments, there is also passive clamped-on current probe (CP), which is applied by authors in [19] to measure power converter common mode and differential mode currents. The advantage of the CP is that it has a large bandwidth up to several hundreds megahertz, however, the CP is usually bulky, which brings an inevitable insertion impedance in the power converter. There are smaller clamp-on CPs, but they can not be generally opened, which is not practical in use.

To adapt to fast switching current measurement, using a current surface probe (CSP) is proposed in this letter. The dimension of the used CSP in comparison with other current

TABLE I: Characteristics of different current measurement equipments

Current Surface Probe (CSP)	Current Probe (CP)	Hall Effect Current Probe (HECP)	Current Shunt (CS)
FCC F-96, 1MHz-450MHz	FCC F-33-3, 1kHz-200MHz	Lecroy CP030, DC-50MHz	SDN-414-025, DC-1.2GHz

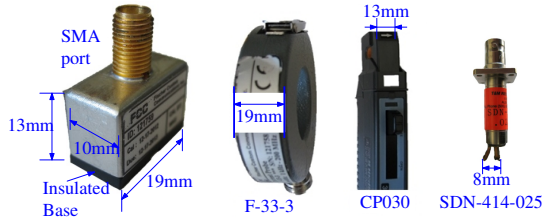


Fig. 1: Dimension of different current probes

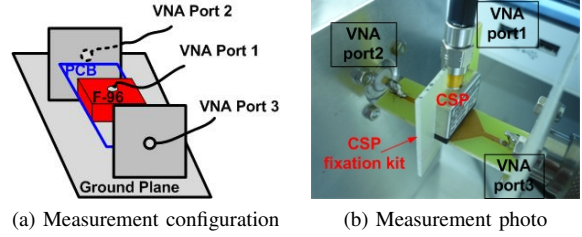


Fig. 2: CSP transfer impedance measurement configuration

probes is shown in Fig. 1 and their characteristics are given in TABLE I. The CSP is a passive probe that allows measuring currents on metallic conductors (PCB track), which is easy to be put and removed from the power converter. An insulated base at one end of the probe helps to provide a galvanic isolation with the conductor, so that the probe can contact directly with the surface over which the current flows. At another end, it is an SMA port.

In this letter, in section II, the current measurement method by CSP is presented. As CSP is a passive probe, its complex transfer impedance is characterized and further verified by comparing the measured IGBT collector switching current together with a passive current probe (CP) and an HECP, of which the dimensions are shown in Fig. 1. In section III, to measure the fast transistor switching current, a GaN-HEMT drain current waveform is measured and compared between the CSP and a CS shown in Fig. 1. The GaN-HEMT drain-source voltage  $V_{DS}$  is measured to demonstrate the influence of the CSP insertion impedance on voltage waveforms. Conclusions are followed after these measurement results in section IV.

## II. CURRENT MEASUREMENT METHOD BY CSP

### A. CSP Transfer impedance characterization

The method proposed by authors in [20], [21] is adapted in this study to determine the CSP transfer impedance with the use of a Vector Network Analyzer (VNA) (Agilent E5071C) on 3 ports. The measurement configuration is illustrated in Fig. 2(a) and the implementation of the CSP is shown in Fig. 2(b). Due to CSP dimension (Fig. 1) and its special half clamp-on structure, its transfer impedance is suspected to be dependent on PCB geometry. For this reason, three PCB configurations, shown in Fig. 3, are designed in the aim of studying the PCB geometry influence on CSP transfer impedance. The width of all PCBs is 19mm which equals to the CSP width.

The transfer impedance characterization helps to get not only the impedance but also the phase information, which is not generally given in current probes technical datasheets. Hence, the CSP complex transfer impedance can be used to compensate its measured current amplitude in frequency domain. Then, the compensated current amplitude can be

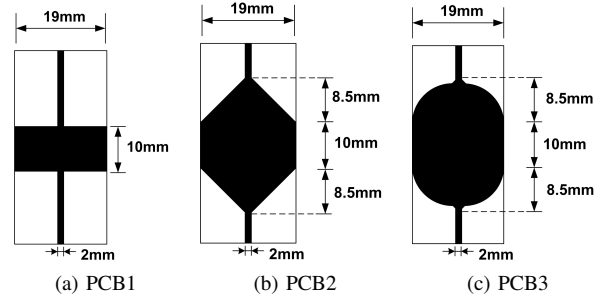
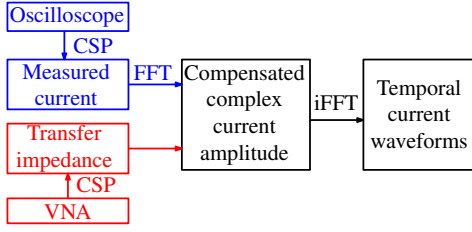


Fig. 3: Three PCB configurations to characterize CSP transfer impedance

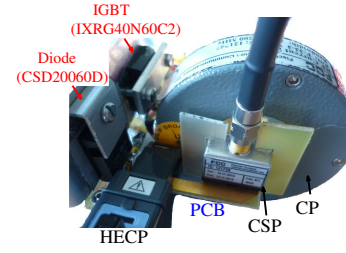
converted into time domain via iFFT to have temporal current waveforms. The flowchart is shown in Fig. 4(a).

The complex transfer impedance measurement results are shown in Fig. 4(b). Above 100MHz, there is a phase shift from  $-180^\circ$  to  $+180^\circ$ , which shows a signal delay due to the N-SMA cable connecting CSP to the VNA. From 10MHz to 200MHz, the difference between PCB1 and PCB2 is about 1.8dB (which corresponds to 24% difference on the delivered probe voltage, which is notably visible on time-domain waveforms), while that between PCB2 and PCB3 is about 0.4dB (which equals to 5% difference in time domain). This result clearly shows that the CSP transfer impedance depends on the PCB geometry, so it is necessary to keep the PCB in the same configuration both in transfer impedance characterization and in power converter current measurement.

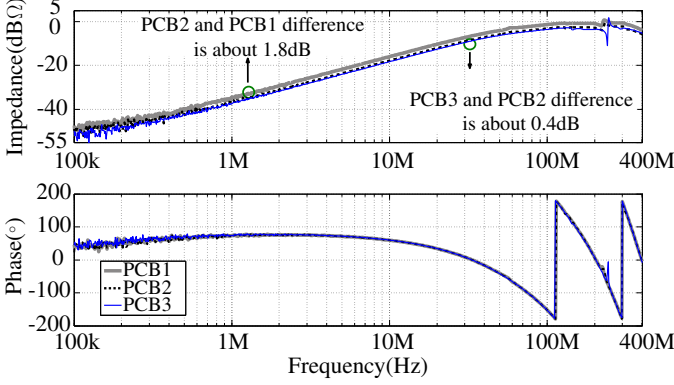
It is shown in Fig. 4b that below 1MHz, the CSP transfer impedance is so small that the characterization results are almost in the noise level, which shows that CSP is suitable for fast switching power devices when power converter switching frequency can arrive to several megahertz. The best measurement sensibility is achieved within the 3dB bandwidth, which is estimated above 50MHz in Fig. 4c. This corresponds to an approximate current switching time less than 6ns, which confirms that CSP is adapted to measure fast switching current.



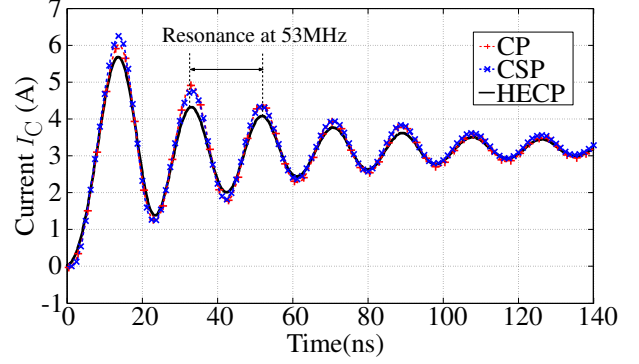
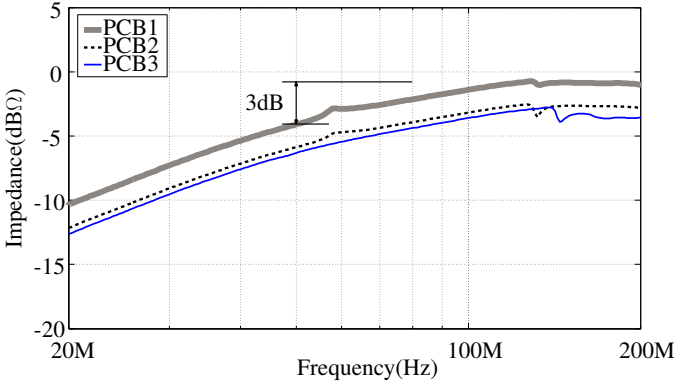
(a) Flowchart



(a) Measurement photo



(b) CSP complex transfer impedance measurement results

(b)  $I_C$  at turn-on

(c) Zoom on 20MHz-200MHz range

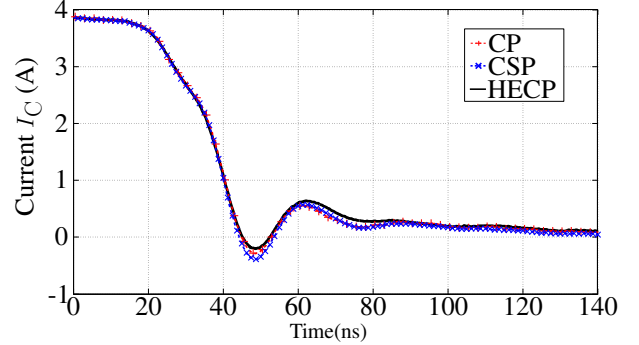
(c)  $I_C$  at turn-off

Fig. 4: Flowchart and CSP complex transfer impedance measurement results

### B. IGBT collector current measurement

In order to validate the obtained results, all the aforementioned current probes are used with a buck converter (Fig. 5(a)) to measure IGBT collector current simultaneously. The width of the PCB connecting the diode anode to the IGBT collector is 19mm. The CSP transfer impedance based on PCB3 is used to compensate CSP measured current, while CP transfer impedance is characterized with the same method.

As CSP and CP transfer impedances are characterized until 400MHz and 200MHz respectively, the converted currents in time domain are sampled at 800MHz and 400MHz individually.

The measured waveforms of the collector current at turn-on and turn-off are shown in Fig. 5(b)(c). As shown in these results, the current measured by CSP and CP in time domain corresponds to the current measured by HECP. Furthermore, the same collector peak current and oscillation frequency

Fig. 5: IGBT current waveform measurement configuration and results

(53MHz) amplitude shown in Fig. 5(b) are measured both by CSP and CP, which are about 20% superior to those measured by HECP due to the attenuation in HECP transfer function above 50MHz. This result proves the validity of the CSP transfer impedance characterization results. Otherwise, if CSP transfer impedance characterization based on PCB1 or PCB2 were used, a 24% or 5% difference would be observed between CSP and CP in the measured current. The CSP current measurement method presented in Fig. 4(a) and its transfer impedance characterization results in Fig. 4(b) can be validated by these measurement results.

### III. GAN-HEMT DRAIN SWITCHING CURRENT MEASUREMENT

In this section, the CSP is compared with a CS to measure the GaN-HEMT fast switching current. It is to be noted that because of its large bandwidth, the CP is able to measure switching current during several nanoseconds. However, the big dimensions of CP shown in Fig. 1 create a long current

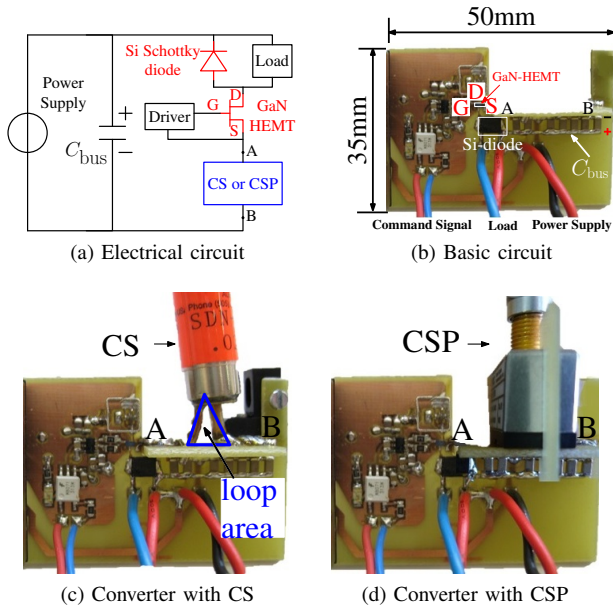


Fig. 6: GaN-HEMT buck converter with two current probes

loop in the measurement circuit, which has a consequence to increase parasitic inductances of the power circuit. The comparison of CSP and CP on fast switching current measurement has been reported by authors in [22].

#### A. GaN-HEMT power converter

To measure fast switching current, with the electrical circuit shown in Fig. 6(a), a buck converter using a GaN-HEMT (EPC2012) and Si-Schottky diode (MBRS3200T3G) is realized with the PCB shown in Fig. 6(b). The GaN-HEMT drain current ( $I_D$ ) flows from the source “S” of the power transistor to the negative terminal “-” of the DC bus capacitors, which are indicated as point A and point B respectively. Therefore, to measure the drain current, either CS or CSP is connected from point A to point B. The measurement setup of each current probe is shown in Fig. 6(c)(d).

In order to realize GaN-HEMT fast switching, it is important to keep the commutation mesh as small as possible to have less parasitic inductances  $L_{para}$ . Therefore, CS and CSP insertion impedances are compared firstly. The insertion impedance of the CS mounted on a PCB using to connect point A and point B (Fig. 6(c)) is characterized directly with an impedance analyzer (IA) (HP4294A). The insertion impedance of the CSP is measured in the following steps: firstly, the impedance of a PCB connecting point A and point B is measured by the IA. Then, the CSP is fixed above the PCB with one end connected to a  $50\Omega$  termination resistor via an N-SMA cable and the shielding part of the cable is connected to the Guard of the impedance analyzer. Thus, the impedance of the PCB with CSP is measured. The measurement configuration and its realization are shown in Fig. 7.

The measurement results are shown in Fig. 8. It can be seen that, the insertion impedance (equivalent to  $L_{para}$ ) induced in the measurement power circuit when using CS is about

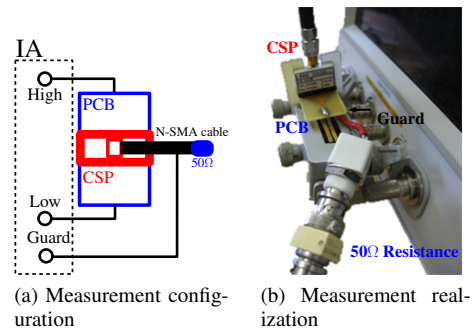


Fig. 7: CSP insertion impedance measurement configuration and its realization

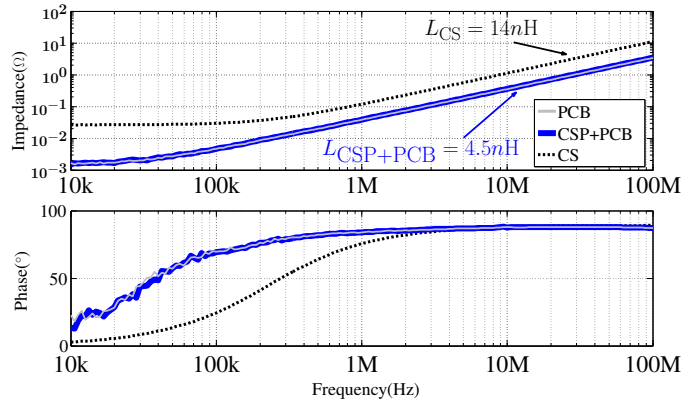


Fig. 8: CS and CSP insertion impedance measurement results

14nH (which is mainly due to the connection pins and internal parasitic inductance of the CS itself [17], [23]) and when using CSP together with the PCB is about 4.5nH. These results show that the use of the CSP brings even less  $L_{para}$  in the measurement circuit than CS. Furthermore, it can be seen in Fig. 8 that the  $L_{para}$  of the PCB alone and the PCB with the CSP is almost the same, which means that the insertion impedance of the CSP is much less than 1nH. This advantage of the CSP guarantees that it has almost no influence on measurement configuration.

#### B. GaN-HEMT drain current measurement

The side view from left side to right side in Fig. 6(c) can be further expressed in Fig. 9(a) when the CSP is used to measure drain current. In Fig. 9(a), it can be seen that the  $I_D$  return current to the negative terminal of the  $C_{bus}$  flows under the PCB. This design is to minimize  $L_{para}$  in the power devices switching mesh when using CSP, however it may modify CSP transfer impedance, because the return current may generate a magnetic field in opposite direction with that generated by the current flowing over the PCB track, so as to reduce the total magnetic field captured by the CSP, thus to reduce CSP transfer impedance. For this reason, the influence of the return current on CSP transfer impedance needs to be considered. Therefore, different like the measurement configuration shown in Fig. 2 in which the influence of the return current can not be characterized, another measurement configuration will be used

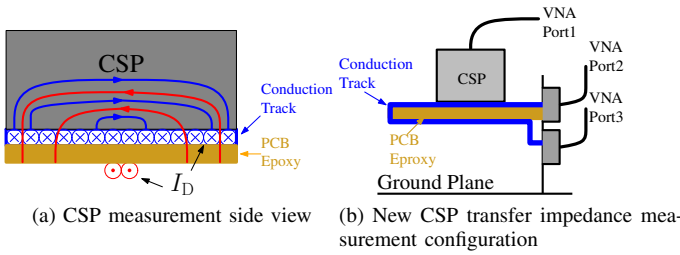


Fig. 9: CSP measurement side view and new transfer impedance measurement configuration

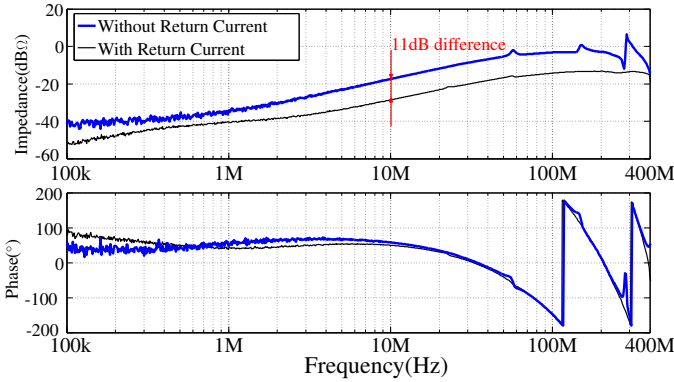


Fig. 10: CSP transfer impedance measurement results without and with the return current

as illustrated in Fig. 9(b). Here, a return current flows under the PCB, thus its influence on CSP transfer impedance can be characterized. The CSP transfer impedance without and with the return current under the PCB is compared in Fig. 10. The dimension of the PCB in the two measurements is the same as that used in the power converter.

It can be seen in Fig. 10 that the maximal CSP transfer impedance difference of both cases above 10MHz can arrive at about 11dB, which puts in evidence the influence of the return current on CSP transfer impedance. If this phenomenon is not taken into consideration, then a huge difference will appear on the transistor switching current waveform measured by CSP.

It is to be noted that even though CSP transfer impedance is degraded in this condition, it reaches 200mΩ above 100MHz (about -14dBΩ), which makes it satisfactory for accurate measurements at high frequency. Still it is important to research on its sensitivity on lateral displacement and angular rotation. For this reason, its transfer impedance is characterized by displacing the CSP from the center of the PCB track with  $\pm 2\text{mm}$  and by rotating from the center with  $\pm 20^\circ$ .

The measurement results of its transfer impedance ( $Z_t$ ) sensitivity on lateral displacement ( $dZ_t/dx$ ) and on angular rotation ( $dZ_t/d\theta$ ) are shown in Fig. 11, in which  $dZ_t/dx$  is less than 1dBΩ/mm and  $dZ_t/d\theta$  is much less than 0.1dBΩ/degree. Furthermore, during all the measurements, the standard derivation of  $Z_t$  is less than 1dBΩ from 10MHz to 100MHz, which shows that CSP  $Z_t$  is only little influenced by imprecise centering on the PCB track.

The power converter switching condition is double-pulse test. The width of the pulse is controlled to have a switching

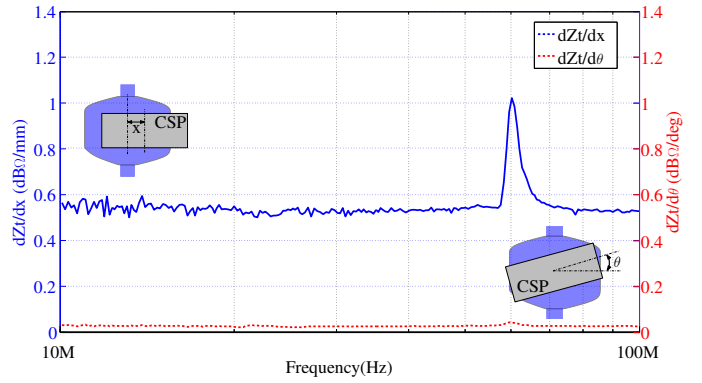
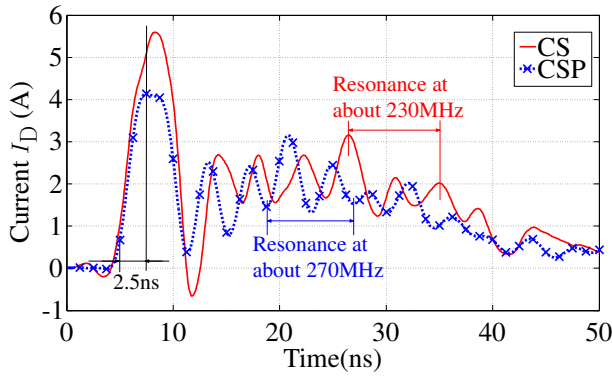


Fig. 11: CSP transfer impedance sensitivity on lateral displacement and angular rotation

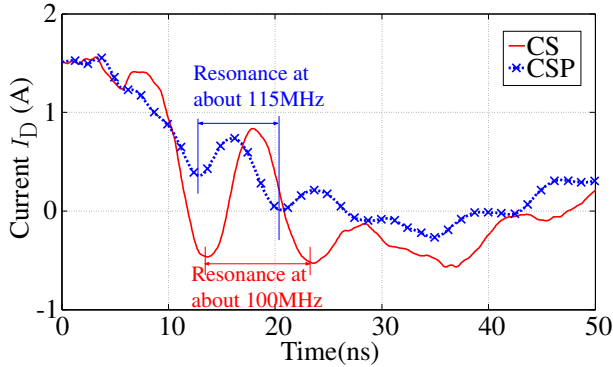
current about 1.5A. The switching voltage ( $V_{DS}$ ) is 50V. In the turn-on switching current shown in Fig. 12(a), the measured current rise time by CSP and CS is almost the same, which is about 2.5ns. An almost same resonance amplitude above 200MHz at the end of the turn-on switching is represented both by CSP and CS. In the turn-off switching current shown in Fig. 12(b), except for the resonance amplitude at around 100MHz, the current waveform measured by CSP is similar to that measured by CS. All the above results prove that CSP is able to measure the fast switching current of a few nanoseconds as well as the CS, and its transfer impedance characterization results presented in Fig. 10 can be validated. It is also shown in this result that the decrease of  $Z_t$  has little influence on measurement accuracy.

The main difference between the measured current waveforms is that there is more peak current amplitude measured by CS than CSP both in turn-on and turn-off switchings. This difference is mainly due to the difference in current measurement circuit of CS and CSP. It is to be noted that in Fig. 6(b), the CS creates a loop area which might capture the high frequency interferences. As shown in the resonance frequency in Fig. 12, that measured by CS is lower than that measured by CSP, which shows more parasitic inductances brought by the CS than CSP in the power device switching mesh, thus it gives rise to more current resonance amplitude. CS and CSP could be simultaneously inserted in the power converter to measure the exact same switching current, however,  $L_{para}$  would be increased in the GaN-HEMT switching mesh and it might slow down the current transition times in this situation.

The  $L_{para}$  difference in the power converter when using CS and CSP can be also demonstrated by measuring turn-off voltage waveform. For this reason,  $V_{DS}$  is measured by a passive voltage probe (VP) (Lecroy PPE4kV, DC-400MHz) in the following conditions: first case, there is CS and VP in the measurement circuit, which is shown in Fig. 13(a). VP also brings the connection of the ground of the oscilloscope in the measurement circuit, thus, it is necessary that the reference point of the VP and the CS is the same point in the power converter due to this inconvenience. Second case, there is CS and VP in the measurement circuit, which is shown in Fig. 13(b). Third case, there is only VP in the measurement circuit, which is shown in Fig. 13(c).



(a)  $I_D$  at turn-on



(b)  $I_D$  at turn-off

Fig. 12: GaN-HEMT switching current measurement results by two probes

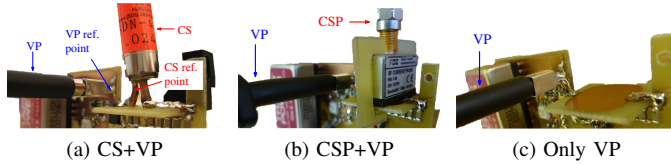
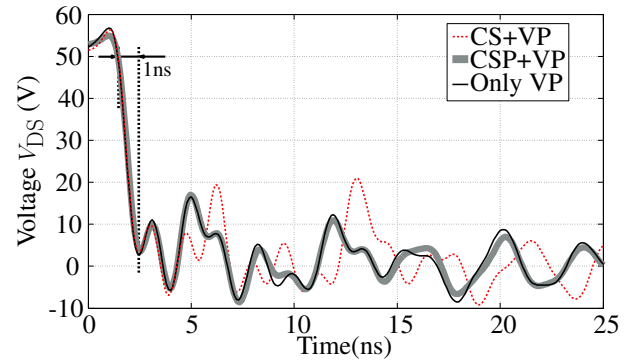


Fig. 13: GaN-HEMT  $V_{DS}$  switching voltage measurement

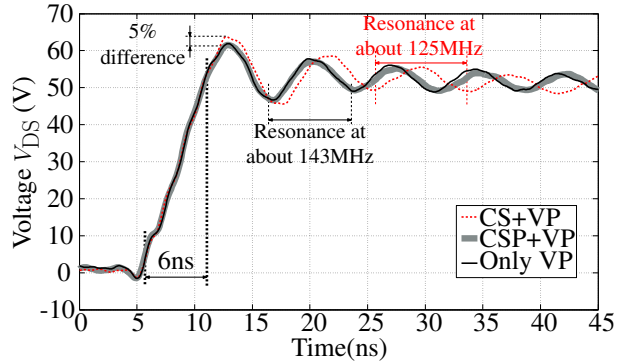
The measured  $V_{DS}$  switching voltage waveforms at each condition are shown in Fig. 14. It can be seen in Fig. 14(b) that the use of CS causes 5% more  $V_{DS}$  turn-off surge voltage than CSP for a voltage rise time of about 6ns. This difference will be further increased if the voltage switching time is further shortened. The use of CS also causes a lower turn-off resonance frequency than that of CSP. The above results prove that the use of CSP brings less  $L_{para}$  than CS in the measurement power circuit, which confirms the current measurement difference observed in Fig.12. It can be also observed that the use of CSP does not modify  $V_{DS}$  voltage waveforms, even in the case that the  $V_{DS}$  turn-on switching time is about 1ns. This result confirms the measurement results in Fig. 8 that the advantage of the CSP is that it brings almost no insertion impedance in the measurement circuit.

#### IV. CONCLUSION

This letter introduces a current measurement method based on current surface probe for the fast switching power semiconductor devices. With the advantage of small dimension



(a)  $V_{DS}$  at turn-on



(b)  $V_{DS}$  at turn-off

Fig. 14: GaN-HEMT  $V_{DS}$  switching voltage measurement results

and isolation, current surface probe allows to have a small commutation mesh in the power circuit while bringing no connection to the ground of the oscilloscope in the power converter through the measurement equipment. Its transfer impedance is first characterized on different PCBs to show its dependency on track dimensions. This study shows that it is necessary to characterize the CSP transfer impedance on the PCB that will be used to measure the current in the power converter. Then, the CSP complex transfer impedance is used to compensate its measured current in frequency domain, and then the compensated current amplitude is converted into time domain via iFFT to have temporal current waveforms. By comparing IGBT collector switching current waveform measured by CP and HECF, the CSP transfer impedance characterization is validated.

Furthermore, the CSP and CS are further compared to measure fast switching current of the GaN-HEMT. A buck converter is designed to minimize parasitic inductances in order to shorten switching times. It is shown that the CSP transfer impedance can be modified when there is a return current under the PCB where the CSP is mounted. By taking this phenomenon into consideration, the converted drain switching current is verified by comparing with the CS. The difference of the measured current is mainly due to the different parasitic inductances when using CS and CSP, which is further confirmed by measuring  $V_{DS}$  switching voltage. It is also shown that the CSP insertion impedance is so small that the use of it has no influence on  $V_{DS}$  switching voltage

measurement.

Finally, as CS brings the ground of the oscilloscope into the measurement circuit, special care is necessary when using other grounded measurement devices. Contrary to that, the CSP has the advantage of keeping the current measurement isolated from the power converter. A common mode loop is introduced in the circuit by the ground connection through the CS, and it may modify the common mode current paths. Future communications will be focused on this aspect on current measurement of the high frequency GaN power converter.

## REFERENCES

- [1] Wu, Y.-F. and Gritters, J. and Shen, L. and Smith, R.P. and Swenson, B., “kV-Class GaN-on-Si HEMTs Enabling 99% Efficiency Converter at 800V and 100kHz,” *Power Electronics, IEEE Transactions on*, vol. 29, pp. 2634–2637, June 2014.
- [2] S. Ji, D. Reusch, and F. Lee, “High-Frequency High Power Density 3-D Integrated Gallium-Nitride-Based Point of Load Module Design,” *Power Electronics, IEEE Transactions on*, vol. 28, no. 9, pp. 4216–4226, 2013.
- [3] X. Huang, Z. Liu, Q. Li, and F. Lee, “Evaluation and Application of 600 V GaN HEMT in Cascode Structure,” *Power Electronics, IEEE Transactions on*, vol. 29, no. 5, pp. 2453–2461, 2014.
- [4] H. Sarnago, O. Lucia, A. Mediano, and J. Burdio, “Design and Implementation of a High-Efficiency Multiple-Output Resonant Converter for Induction Heating Applications Featuring Wide Bandgap Devices,” *Power Electronics, IEEE Transactions on*, vol. 29, no. 5, pp. 2539–2549, 2014.
- [5] R. Mitova, R. Ghosh, U. Mhaskar, D. Klikic, M.-X. Wang, and A. Dentella, “Investigations of 600-V GaN HEMT and GaN Diode for Power Converter Applications,” *Power Electronics, IEEE Transactions on*, vol. 29, no. 5, pp. 2441–2452, 2014.
- [6] M. Rodriguez, Y. Zhang, and D. Maksimovic, “High-Frequency PWM Buck Converters Using GaN-on-SiC HEMTs,” *Power Electronics, IEEE Transactions on*, vol. 29, no. 5, pp. 2462–2473, 2014.
- [7] J. Valle-Mayorga, C. Gutshall, K. Phan, I. Escorcia-Carranza, H. Mantooth, B. Reese, M. Schupbach, and A. Lostetter, “High-Temperature Silicon-on-Insulator Gate Driver for SiC-FET Power Modules,” *Power Electronics, IEEE Transactions on*, vol. 27, pp. 4417–4424, nov. 2012.
- [8] Z. Xu, D. Jiang, M. Li, P. Ning, F. Wang, and Z. Liang, “Development of Si IGBT Phase-Leg Modules for Operation at 200°C in Hybrid Electric Vehicle Applications,” *Power Electronics, IEEE Transactions on*, vol. 28, no. 12, pp. 5557–5567, 2013.
- [9] M. Danilovic, Z. Chen, R. Wang, F. Luo, D. Boroyevich, and P. Mattavelli, “Evaluation of the switching characteristics of a Gallium-Nitride transistor,” in *Energy Conversion Congress and Exposition (ECCE), 2011 IEEE*, pp. 2681–2688, sept. 2011.
- [10] X. Huang, Q. Li, Z. Liu, and F. Lee, “Analytical Loss Model of High Voltage GaN HEMT in Cascode Configuration,” *Power Electronics, IEEE Transactions on*, vol. 29, no. 5, pp. 2208–2219, 2014.
- [11] J. Wang, H. S.-h. Chung, and R. T.-h. Li, “Characterization and Experimental Assessment of the Effects of Parasitic Elements on the MOSFET Switching Performance,” *Power Electronics, IEEE Transactions on*, vol. 28, pp. 573–590, jan. 2013.
- [12] F. Costa, E. Labouré, F. Forest, and C. Gautier, “Wide bandwidth, large AC current probe for power electronics and EMI measurements,” *Industrial Electronics, IEEE Transactions on*, vol. 44, pp. 502–511, Aug 1997.
- [13] S. Ziegler, R. Woodward, H.-C. Iu, and L. Borle, “Current Sensing Techniques: A Review,” *Sensors Journal, IEEE*, vol. 9, pp. 354–376, April 2009.
- [14] P. Poulichet, F. Costa, and E. Laboure, “A new high-current large-bandwidth DC active current probe for power electronics measurements,” *Industrial Electronics, IEEE Transactions on*, vol. 52, pp. 243–254, Feb 2005.
- [15] W. Ray and C. Hewson, “High performance Rogowski current transducers,” in *Industry Applications Conference, 2000. Conference Record of the 2000 IEEE*, vol. 5, pp. 3083–3090 vol.5, 2000.
- [16] Zhengyang Liu and Xiucheng Huang and Lee, F.C. and Qiang Li, “Package Parasitic Inductance Extraction and Simulation Model Development for the High-Voltage Cascode GaN HEMT,” *Power Electronics, IEEE Transactions on*, vol. 29, pp. 1977–1985, April 2014.
- [17] R. Robutel, C. Martin, C. Buttay, H. Morel, P. Mattavelli, D. Boroyevich, and R. Meuret, “Design and Implementation of Integrated Common Mode Capacitors for SiC-JFET Inverters,” *Power Electronics, IEEE Transactions on*, vol. 29, pp. 3625–3636, July 2014.
- [18] Laimer and Kolar, “Accurate Measurement of the Switching Losses of Ultra High Switching Speed CoolMOS Power Transistor/SiC Diode Combination Employed in Unity Power Factor PWM Rectifier Systems,” in *Proc. 8th European Power Quality Conference (PCIM)*, pp. 71–78, 2002.
- [19] X. Gong and J. Ferreira, “Comparison and Reduction of Conducted EMI in SiC JFET and Si IGBT-Based Motor Drives,” *Power Electronics, IEEE Transactions on*, vol. 29, no. 4, pp. 1757–1767, 2014.
- [20] G. Cerri, R. De Leo, V. Primiani, S. Pennesi, and P. Russo, “Wide-band characterization of current probes,” *Electromagnetic Compatibility, IEEE Transactions on*, vol. 45, no. 4, pp. 616–625, 2003.
- [21] C. Cuellar, N. Idir, A. Benabou, and X. Margueron, “High frequency current probes for common-mode impedance measurements of power converters under operating conditions,” in *Power Electronics and Applications (EPE), 2013 15th European Conference on*, pp. 1–8, 2013.
- [22] K. Li, A. Videt, and N. Idir, “GaN-HEMT fast switching current measurement method based on current surface probe,” in *Power Electronics and Applications (EPE’14-ECCE Europe), 2014 16th European Conference on*, pp. 1–10, Aug 2014.
- [23] C. Johnson and P. Palmer, “Current measurement using compensated coaxial shunts,” *Science, Measurement and Technology, IEE Proceedings*, vol. 141, no. 6, pp. 471–480, 1994.